BULK SUBMILLIMETER-WAVE MIXERS: STRAIN AND SUPERLATTICES

M. M. Litvak and H. M. Pickett
Jet Propulsion Laboratory
California Institute of Technology
Pasadena, California 91103

SUMMARY

Strained germanium crystals, doped with gallium, are used as heterodyne mixers at THz frequencies, with IF bandwidths approaching a GHz. The mixer performance (conversion loss and mixer noise) is analyzed in terms of nonlinearities associated with acceptor levels and with relaxation rates of free holes. Comparison is made with similar mixers employing low-lying donor levels in high-purity GaAs and with hot-electron InSb mixers.

INTRODUCTION

Stress has been used to tune the photoconductive response of lightly Ga-doped Ge bolometers in the far infrared over the range 50 to 100 cm^{-1} (100 to 200 μm)(ref. 1).

The degeneracy of the valence band edge (fig. 1) and of the acceptor ground levels is lifted by the strain (ref. 2). The acceptor binding energy decreases with compressive strain (ref. 3). The split-off component of the band edge that is higher in the gap dominates the character of the hole motion. That is, for large strains the acceptor ground level wave function is a superposition of wave functions for the energy-raised part of the valence band. The effect of the wave functions of the energy-lowered part is small for stresses approaching 10^4 kg/cm^2. For somewhat weaker stress, the binding energy is given by $\varepsilon(S) = \varepsilon_o + \varepsilon_1/S$, where ε_o = 4.9 meV, ε_1 = 8.64 eV-kg/cm^2 and S is the stress in kg/cm^2.

The mechanism for mixing in n-InSb is the power dependence of the mobility (ref. 4). The mobility is temperature dependent, mainly due to momentum-changing collisions of electrons with ionized impurities. The temperature increases with the absorbed power. This power contains the usual contribution that oscillates at the beat frequency between the signal and local-oscillator frequencies. The response time is the energy relaxation time of hot electron energy to the lattice, which time is 10^{-7}s. This corresponds to an IF bandwidth of ~3 MHz (FWHM).

Extensive far-infrared spectroscopy (ref. 5) and mixing experiments (ref. 6) have been done in high-purity n-GaAs. The main mechanism for mixing has been via the modulation of the density of conducting electrons upon

photoionization of the low-lying donor levels. This photoionization might arise from a two-step process of photoexcitation to an excited, bound level of the donor, followed by rapid thermal (or near thermal) ionization by acoustic phonons at 4K, with little carrier heating. The time response is the capture relaxation time of the conduction electrons by the ionized donors, which time is 10^{-8}s (about ten times shorter than for InSb). This corresponds to an IF bandwidth of 30 MHz (FWHM). This time and bandwidth depend upon the density of capture centers, as determined by the doping, the degree of compensation, the temperature, and the amount of photoionization.

Heterodyne mixing between the signal and local oscillator (LO) at THz (10^{12} Hz) frequencies is detected in the photocurrent collected with an applied bias voltage. The mixing is accomplished mainly through modulation of the free-carrier density. The free carriers appear from the photoionization of the impurity ground level. For acceptors (Ga), the bound holes are excited to the valence band by absorption of the combined signal to be measured and the LO. See fig. 2. The modulation has a frequency (IF) equal to the difference of frequencies of these two sources.

The depth of modulation rapidly decreases when the IF (in s^{-1}) exceeds the inverse-response time of the carrier density. This response time is mainly the hole capture (recombination) time owing to ionized acceptors. The Coulomb-like capture cross sections are very large at low temperatures. Compensation by donors assures the presence of ionized acceptors despite the tendency for carrier freezeout. Higher degrees of compensation and higher LO power increase the number of capture centers and, thus, the inverse-response time, which is the FWHM IF bandwidth (divided by π).

MIXING MECHANISM

The photocurrent waveform in the crystal is the current density, $\underline{j}(t)$, integrated over the cross-sectional area. Assuming carriers of only one type for simplicity, $\underline{j}(t) = e\, n(t)\, \underline{v}(t)$, where n and $\underline{v}$ are the number density and velocity of the carriers. Then, in the small-signal limit, the current can be modulated at the IF under three circumstances, i.e., the density can be modulated at the IF, the velocity can be modulated at the IF, or one is modulated at the LO frequency and the other at the signal frequency. A dc bias current is also present. Modulation of the density, the first case, is mainly caused by the square-law dependence on total incident electric field E(t), i.e., LO plus signal, $\underline{E}(t) = 1/2\, [\underline{E}_L \exp(-i\omega_L t) + \underline{E}_1 \exp(-i\omega_1 t)]$ + complex conjugate, through the rate of photoionization in p-Ge (Ga), or photo-excitation/ionization in n-GaAs, or free-carrier absorption in n-InSb. Modulation of the velocity, the second case, can occur through temperature dependence of the mobility or through nonparabolic-band effects. The third case, modulating density and velocity each at high frequency, really coresponds to a displacement current density. Only the first case, modulation of the carrier density, appears capable of both good sensitivity and large bandwidth. Modulation of the velocity through the mobility is the hot electron mechanism of n-InSb, while the other mechanisms appear too weak (ref. 7).

The equation for the carrier density n in excess over dark conditions is

$$\frac{\partial n}{\partial t} + \underline{\nabla} \cdot n\underline{v} = \dot{n} - \frac{n}{\tau}$$

where $\dot{n}$ is the volume rate for carrier photogeneration and τ is the carrier recombination time. The dominant component at the IF for the current density is given by

$$\underline{j}_o = \frac{e\,\underline{\underline{\mu}} \cdot \underline{E}_{dc}\,\tau}{1 - i\omega_o \tau} \quad \frac{\alpha\,\underline{E}_L \cdot \underline{E}_1 c}{4\pi\hbar\,|\omega_L \omega_1|^{1/2}}$$

where $\underline{\underline{\mu}}$ denotes the mobility tensor in the presence of uniaxial strain, $\underline{E}_{dc}$ is the bias field and α is the absorption coefficient (cm^{-1}) at the LO or signal frequency, the distinction being neglected. Quantities associated with the IF, LO, and signal frequencies are denoted by subscript o, L, and 1, respectively.

Conversion Loss

The intrinsic conversion loss L' is the ratio of the absorbed signal power to the IF power associated with the above current density, i.e.,

$$L' = \int d^3r\ \alpha |\underline{E}_1|^2 \frac{c}{8\pi} \Big/ \int d^3r\ |j_o|^2 / 2\sigma_o$$

where σ_o is the IF conductivity and the integrals are over the crystal volume. See fig. 3 for the geometry being used. Thus,

$$L' = \frac{\left(1 + \omega_o^2 \tau^2\right) R_o}{2\, P_L \mathscr{R}^2 \eta} \tag{1}$$

where the responsivity $\mathscr{R} = GeR_o/\hbar|\omega_L\omega_1|^{1/2}$ (volts/watt) and the photoconductive gain $G = \tau/\tau_d$, where $\tau_d = \ell/\mu E_{dc}$, is the drift time along the crystal length ℓ. The power $P_L = E_L^2\, c\ell w/8\pi$, where w is the width (see fig. 3). The efficiency factor η accounts for absorption and surface impedance-mismatch. The conversion loss L based on power delivered to an IF load resistance $R_{o,e}$ is obtained by multiplying L' by $(R_o + R_{o,e})^2/R_o R_{o,e}$ (ref. 4).

The conversion loss for InSb is a similar expression as for L', when the responsivity, $\mathscr{R}$, is set equal to the following (ref. 4): $\mathscr{R} = [GeR_o/(3kT_e/2)]$ $(d\ \ell n\ R_o/d\ \ell n\ T_e)$ and when τ is replaced everywhere by τ_ε, the hot electron-temperature (T_e) relaxation time. With the same absorption efficiencies η

for the Ge- and InSb-cases, the conversion losses will be in the inverse square of the ratio of the responsivities. Since this responsivity ratio is $(\tau/\tau_\varepsilon)(3kT_e/2\hbar\omega_L)/(d\ \ell nR_o/d\ \ell nT_e)$ and since the first two factors are considerably smaller than unity, and the third factor is approximately unity, the higher conversion loss for Ge is evident. Note that the product GR_o in the formula for either responsivity is independent of the mobility and the crystal length. However, L' is proportional to R_o, in equation (1), which makes L' vary inversely with the mobility. The responsivity for $Hg_{0.8}\ Cd_{0.2}\ Te$ is reported (ref. 8) to be 15 times higher than InSb, owing to a larger logarithmic derivative of the resistance when a magnetic field induces a transport anomaly at low temperature. As seen in equation (1), the IF response has a half-width at half-maximum equal to τ^{-1}, where τ is the effective recombination time. As the LO power is increased, this bandwidth is also increased, owing to the appearance of additional ionized acceptors which have large capture cross-sections.

Polarization Dependence

The ground acceptor level and the uppermost valence band edge have J = 3/2, $M_J = \pm 1/2$ for angular momentum quantum numbers. The electric dipole line-strengths for the two orthogonal senses of linear polarization (parallel and perpendicular to the uniaxial stress) are proportional to:

$$S_K = (2J + 1)^2 \begin{pmatrix} J & 1 & J \\ -M_J & K & M_J - K \end{pmatrix}^2 \varepsilon_K$$

where, in the Wigner 3-J symbol (ref. 9) K = 0 for parallel polarization, K = 1 for perpendicular linear polarization, $\varepsilon_o = 1$ and $\varepsilon_1 = 1/2$. Then $S_o = 4/15$ and $S_1 = 16/15 = 4S_o$. Thus, polarization perpendicular to the stress is preferred by the relative line strengths by a factor of four. The electric dipole moment squared for absorption along either direction is also proportional to the square of the inverse-mass component for that direction. Since the ratio of perpendicular-to-parallel mass (ref. 3) is 2.5 for stress in the [100] direction (and 3.2 for a [111] stress direction), the mass dependence more than offsets the above line-strength preference.

Noise Characteristics

Mixer IF noise consists mainly of thermal noise associated with dissipative processes, shot noise associated with the current produced by the LO, and generation-recombination noise associated with ionization of impurities and capture of carriers.

The thermal noise is mainly caused by carrier-velocity fluctuations $\langle \delta v^2 \rangle = kT/m$, so that the spectral density of current fluctuations in a bandwidth $\Delta\nu$ is given by (ref. 10)

$$\langle \delta I^2_{\omega_n} \rangle / \Delta\nu = \hbar\omega_n \coth\left(\frac{\hbar\omega_n}{2kT}\right) \text{ Re } Y_{nn} ,$$

where Y_{nn} is the total admittance for mixer and external load or terminations. The coth factor includes the zero-point quantum fluctuations. The frequency (s^{-1}) $\omega_n = \omega_o + n\omega_L$, is for the n-th sideband for an LO frequency ω_L and an IF, ω_o.

In general, Y_{mn} is the matrix element of admittance that multiplies the small-signal voltage at frequency ω_n to give the small-signal current at frequency ω_m. Thus,

$$Y_{mn} = G_{m-n} - i\,(\omega_o + m\omega_L)\, C_{m-n}$$

where G_k and C_k are the time-Fourier components of total conductance and capacitance in the presence of the large-signal, periodic, LO electric field (ref. 11) at the frequency ω_L.

Shot noise consists of charge-density fluctuations owing to the discrete particle nature of the carriers. The corresponding noise-Fourier correlation matrix elements are given by

$$\langle \delta I_m \, \delta I_n^* \rangle / \Delta\nu = 2e\, I_{m-n}$$

where I_{m-n} is the (m-n)-th Fourier component of the large-amplitude current waveform i(t) in the presence alone of the LO electric field at ω_L, i.e.,

$$i(t) = \sum_{k=-\infty}^{\infty} I_k \, e^{-ik\omega_L t}$$

The off-diagonal elements represent anomalous noise owing to correlations among the up- and down-converted components of the modulated shot noise, which is proportional to the instantaneous current i(t).

The noise temperature T_M of the mixer is determined by the apparent noise current, acting in the signal sideband alone at the mixer input, that would result in the observed IF noise voltage. This IF noise voltage is mainly the result of thermal noise, LO shot-noise, and generation-recombination (g-r) noise at all sidebands.

If the impedance Z_{ij} is the ij-th matrix element of the inverse of the admittance matrix, then the apparent signal noise current in the bandwidth $\Delta\nu$ is given by

$$\langle \delta I^2_{\omega_1} \rangle / \Delta\nu = \hbar\omega_1 \coth\left(\frac{\hbar\omega_1}{2kT_M}\right) \text{ Re } Y_{11}$$

$$= \text{Re}\left(\sum_{i,j} Z_{oi}\, Z^*_{oj} \langle \delta I_i\, \delta I^*_j \rangle / \Delta\nu\right) / |Z_{01}|^2 \qquad (2)$$

where $\text{Re} \langle \delta I_i\, \delta I^*_j \rangle / \Delta\nu = \delta_{ij}\, \hbar\omega_i \coth\left(\frac{\hbar\omega_i}{2kT}\right) \text{ Re } Y_{ii} + 2eI_{i-j}$ + (g-r) noise

$$Y_{00} \simeq R_o^{-1} + R_{o,e}^{-1}$$

$$Y_{11} \simeq \frac{c}{4\pi}\, \eta\, \frac{\ell}{w} + Y_{1,e}$$

$$Y_{01} \simeq \frac{c}{4\pi}\, \eta\, \frac{eE_L\, \ell}{\hbar |\omega_L \omega_1|^{1/2}}\, \frac{G}{1 - i\omega_o \tau}$$

and

$$Y_{10} \simeq \frac{c}{4\pi}\, \eta\, \frac{eE_L\, \ell}{\hbar |\omega_L \omega_o|^{1/2}}\, \frac{G}{1 - i\omega_1 \tau}$$

The subscripts 0, 1 and L refer to the IF, the signal and the LO, respectively. The admittances with subscript e refer to external loads or terminations, which may be suitably matching. Admittances are in Gaussian units. For practical units, replace $c/4\pi$ by $1/Z_o$, where Z_o is the wave impedance of free space. The factor η is the overall efficiency factor for absorption of the incident radiation, including the factor correcting for surface reflectance.

For no surface reflection and a thin crystal width, $\eta \simeq \alpha w$, where α is the absorption coefficient for acceptor photoionization and w is the width. Equation (2) may be solved then for T_M.

With this admittance formalism, the conversion loss L can be rewritten more generally (ref. 11) as

$$L_{01} = \text{Re}(Z_{00})\, \text{Re}(Z_{11}) / |Z_{01}|^2$$

where the impedance matrix elements are obtained from the inverse admittance matrix, which includes all sidebands together. The image sideband, for example, at ω_{-1} can be expected to have some influence.

The photoconductor density fluctuations due to generation-recombination (g-r) of the carriers is given by $\langle \delta n_h^2 \rangle = \eta P_L \tau/(\text{vol.}^2 \hbar\omega_L)$, where vol. is the crystal volume being illuminated. The g-r noise current is then

$$\langle \delta I_o \, \delta I_o^* \rangle / \Delta\nu = \frac{4e^2 P_L}{\hbar\omega_L} \frac{\eta G^2}{1 + \omega_o^2 \tau^2}$$

This spectral shape (with respect to ω_o) arises from the exponential decay in time, with correlation time τ, of the density fluctuations. This noise source is to be incorporated into the right-hand side of the equation for the mixer temperature, equation (2). Space-charge effects can influence this spectral shape (ref. 10). A particular concern is the plasma resonance near the hole plasma frequency, $\omega_p = (4\pi n_h e^2/m\varepsilon)^{1/2}$. Spatial fluctuations cause charge separation fields between holes and ionized acceptors. The divergence of this field causes a $\nabla \cdot \underline{v}$ - contribution in the equation for the carrier density, resulting in an enhancement of the above fluctuations by a factor $|\varepsilon(\omega_o)|^{-2}$ where

$$\varepsilon(\omega_o) \simeq 1 + \omega_p^2 \Big/ \left(-i\omega_o + \frac{1}{\tau}\right)\left(-i\omega_o + \frac{1}{\tau_p}\right)$$

and τ_p is the mobility relaxation time. These expressions ignore the shielding effects by electrons and the wavevector dependence, involving the Debye lengths. The thermal noise will be enhanced through modification of the IF admittances. Note that the plasma frequency is ~ 1 GHz for $n_h = 10^{11}$ holes/cm^3.

HETEROJUNCTION — SUPERLATTICES

Spatially periodic heterojunctions (e.g., Ge/GaAs) establish walls of adjacent one-dimensional potential wells and barriers. These can favorably affect the hole density of states and collision/capture times in the valence band (refs. 12 and 13). Improved mixer performance results from an increased photoabsorption with a greater density of final states and from decreased thermal noise with decreased dissipation in the IF sideband.

Major improvement would occur with an increased steepness of photocurrent dependence on modulated power. Tunneling through the potential barriers allows an exponential dependence. One means of introducing this dependence is to consider that the power modulation causes a carrier density modulation $\Delta n(t)$ in the Ge doped with Ga. Note that the superlattice acts to lift the degeneracy of the valence band edge much as strain would. The density modulation causes

an electrostatic potential energy $e\phi = 4\pi e^2 a^2 \Delta n(t)/\varepsilon$, where ε is the Ge dielectric constant, and a is the radius of curvature of the band bending (in the Ge potential wells) owing to excess holes near the walls to the adjacent barriers. See figure 4. This potential energy oscillates at the IF, i.e., $\phi = \phi_o \cos \omega_o t$.

This time dependence affects the hole quantum wave functions for the potential wells. The resulting tunneling current ΔI_o at the IF involves the overlap of wave functions for modulated energy levels in the wells, whose energies consistently differ by $\hbar\omega_o$. Thus, in terms given (ref. 14) by the Bessel functions J_n,

$$\Delta I_o \simeq \sum_{n=-\infty}^{\infty} J_n(X) \left[J_{n+1}(X) + J_{n-1}(X) \right] I_{dc}(eV_{dc} + n\hbar\omega_o)$$

where $X = e\phi_o/\hbar\omega_o$ and I_{dc} is the dc current as a function of bias voltage. This function can be an approximate exponential function of bias voltage, which is effectively $(V_{dc} + n\hbar\omega_o/e)$ for the n-photon contribution.

By appropriate spatial modulation of the doping and compensation in the superlattice the carrier lifetime can be shortened to increase the bandwidth, yet the mobility can be increased to reduce the noise and conversion loss. This requires the trapping in the Ge wells to increase capture by the local acceptors but the scatter of the two-dimensional hole gas, especially by impurities in the GaAs barrier regions, to be reduced.

CONCLUSIONS

The mixing mechanism in stressed Ge is similar to that in high-purity GaAs, and leads to larger bandwidths than for hot-electron InSb. Stress allows tunability of the Ge (doped with Ga) in a wavelength range inaccessible to n-GaAs even with magnetic fields.

Superlattices can provide exponential-type IF current-voltage characteristics for greater sensitivity. Spatial modulation of the doping and compensation can increase the bandwidth and the mobility for better performance, i.e., less conversion loss and less noise.

REFERENCES

1. Kazanskii, A. G.; Richards, P. L.; and Haller, E. E.: Far-Infrared Photoconductivity of Uniaxially Stressed Germanium. Appl. Phys. Lett., Vol. 31, 1977, pp. 496-497.

2. Hensel, J. C.; and Feher, G.: Cyclotron Resonance Experiments in Uniaxially Stressed Silicon. Phys. Rev., Vol. 129, 1963, pp. 1041-1062.

3. Hall, J.J.: Large-Strain Dependence of the Acceptor Binding Energy in Germanium, Phys. Rev., Vol. 128, 1962, pp. 68-75.

4. Whalen, J.J.; and Westgate, C.R.: Temperature Dependence of the Conversion Loss and Response Time of InSb Mixers. IEEE Trans. Electron Devices, Vol. ED-17, 1970, pp. 310-319.

5. Stillman, G. E.; Wolfe, C. M.; and Dimmock, J. O.: Detection and Generation of Far Infrared Radiation in High Purity Epitaxial GaAs. Symposium on Submillimeter Waves, Polytechnic Institute of Brooklyn, 1970, pp. 345-359.

6. Fetterman, H.; Tannenwald, P. E.; and Parker, C. D.: Millimeter and Far Infrared Frequency Mixing in GaAs. Symposium on Submillimeter Waves, Polytechnic Institute of Brooklyn, 1970, pp. 591-594.

7. Lao, B. Y.; and Litvak, M. M.: Far-Infrared Mixing in High-Purity GaAs. Journ. Appl. Phys., Vol. 42, 1971, pp. 3357-3360.

8. Nimtz, G.; Schlicht, B.; Lehmann, H.; and Tyssen, E.: A New Sensitive Microwave Bolometer Heterodyne Receiver. Appl. Phys. Lett., Vol. 35, 1979, pp. 640-641.

9. Edmonds, A. R.: Angular Momentum in Quantum Mechanics. (Princeton U, Princeton, 1960) 2nd ed., pp. 45-52.

10. Van Vliet, K. M.; and Fassett, J. R.; Fluctuations due to Electronic Transitions and Transport in Solids. Fluctuation Phenomena in Solids, R. E. Burgess, ed. (Academic: New York, 1965), pp. 267-354.

11. Held, D. N.; and Kerr, A. R.: Conversion Loss and Noise of Microwave and Millimeter-Wave Mixers: Part 1 - Theory. IEEE Trans. Microwave Theory and Techn., Vol. MTT-26, 1978, pp. 49-55.

12. R. Dingle: Confined Carrier Quantum States in Ultrathin Semiconductors in Heterostructures. Festkorperproblem XV, Advances in Solid State physics, H.J. Queisser, ed. (Pergamon-Vieweg: Braunschweig), 1975, pp. 21-48.

13. Hess, K: Impurity and Phonon Scattering in Layered Structures, Appl. Phys. Lett., Vol. 35, 1979, pp. 484-486.

14. Tucker, J. R.; and Millea, M. F., Photon Detection in Nonlinear Tunneling Devices. Appl. Phys. Lett., Vol. 33, 1978, pp. 611-613.

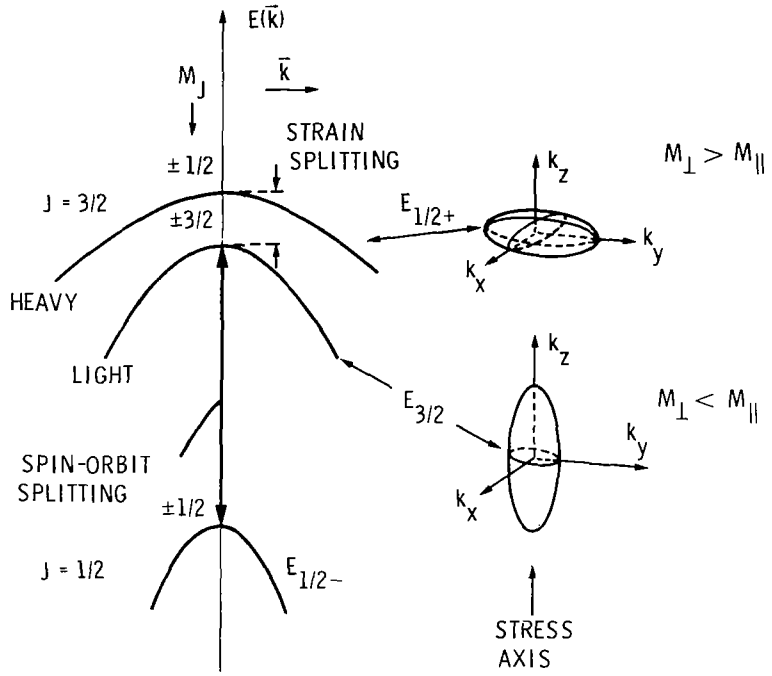

Figure 1.- Split valence bands of uniaxially compressed germanium. Uppermost valence band is heavy hole ($J = 3/2$, $M_J = \pm 1/2$) band with perpendicular mass greater than parallel mass.

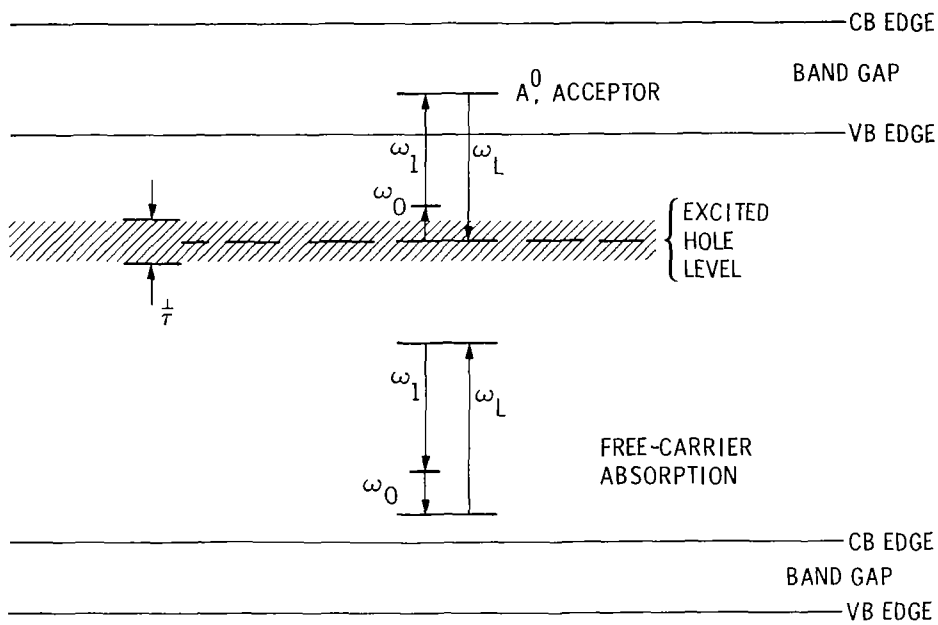

Figure 2.- Nonlinear photoionization process for mixing. Width of individual hole level within valence band (VB) is shown as $1/\tau$, where τ is effective carrier lifetime. Local oscillator (LO) frequency, signal frequency, and intermediate frequency (IF) are ω_L, ω_1, and ω_o, respectively, where $\omega_o = \omega_L - \omega_1$.

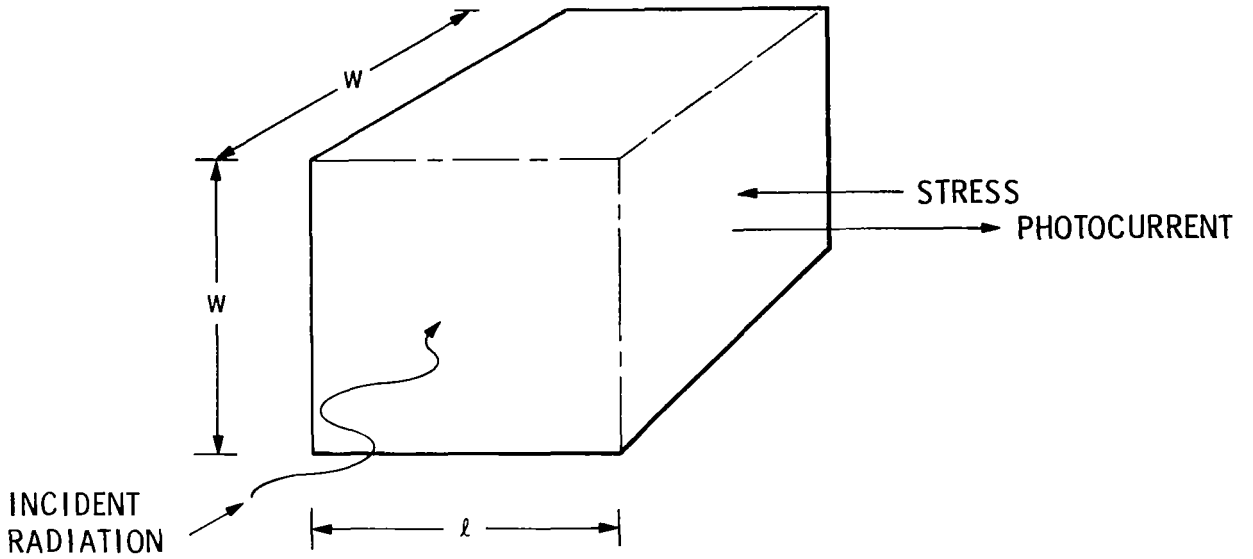

Figure 3.- Crystal geometry and directions for illumination, photocurrent, and uniaxial stress.

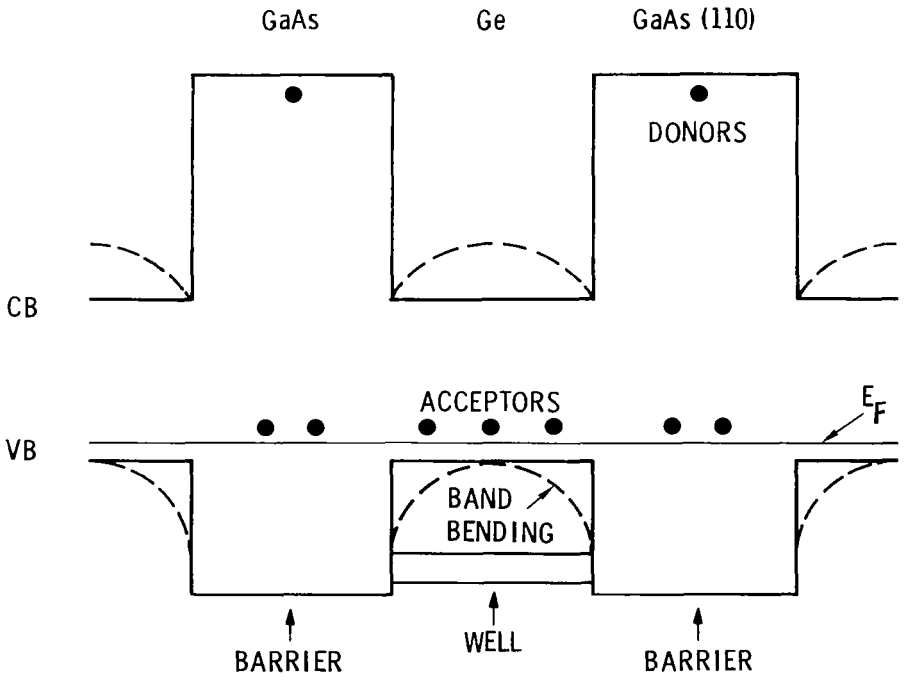

Figure 4.- Energy band diagram for p-Ge/GaAs (110) superlattice.